We are IntechOpen, the world's leading publisher of Open Access books Built by scientists, for scientists

4,800
Open access books available

122,000
International authors and editors

135M
Downloads

Our authors are among the

154
Countries delivered to

TOP 1%
most cited scientists

12.2%
Contributors from top 500 universities

CLARIVATE ANALYTICS BOOK CITATION INDEX INDEXED

WEB OF SCIENCE™

Selection of our books indexed in the Book Citation Index in Web of Science™ Core Collection (BKCI)

Interested in publishing with us?
Contact book.department@intechopen.com

Numbers displayed above are based on latest data collected.
For more information visit www.intechopen.com

Chapter 4

Active Vibration Control Using a Kautz Filter

Samuel da Silva, Vicente Lopes Junior and Michael J. Brennan

Additional information is available at the end of the chapter

http://dx.doi.org/10.5772/50966

1. Introduction

Impulse response functions (IRFs) have been largely used in experimental modal analysis in order to extract the modal parameters (natural frequencies, damping factors and modal forms) in different areas. IRFs occupy a prominent place in applications of aeronautical, machinery and automobile industries, mainly when the system has coupled modes. Additionally, IRFs have practical advantages for use in control theory for many reasons, e.g.:

- For very complex systems, they can be determined by experimental tests, or using data of input and output measured by load cells or accelerometers, or directly with an impact hammer.
- The identified model is essentially nonparametric.
- Normally a finite impulse response (FIR) model of the structure is employed. Thus, the stability can be warranted a priori. Additionally, the many adaptive controlers are based on an FIR structure and it is easy to
  perform a recursive estimation.

In general, IRFs can be identified by impact tests with an instrumented hammer or by using numerical algorithms implemented in commercial software. IRFs can be determined with those algorithms through different methods, e. g., the covariance method based on the sum of convolutions of the measured input forces. However, there is an over parametrization that is a drawback when the lag memory is high. Fortunately, an expansion of the IRFs into orthonormal basis functions can enhance the procedure of reducing the number of parameters [15]. For describing mechanical vibrating systems, Kautz filters are interesting orthogonal functions set in Hilbert space [21] that include a priori knowledge about the dominant poles. The eigenvalues associated to vibrating mechanical systems are conjugated complex poles, so, the IRFs can be expanded in orthonormal basis functions with those conditions. Kautz filters are orthogonal funcions that can be used for this purpose. These filters can decrease the computational cost and accelerate the convergence rate providing a good estimate of the IRFs [14].

Kautz filters have found several applications, e.g., acoustic and audio [20], circuit theory [17], experimental modal analysis in mechanical systems [2, 12–14], vibration control [6], model reduction [4], robust control [18], predictive control [19], general system identification [5, 16, 22, 25], non-linear system identification with Volterra models [7–11], etc. Although it may seem that the mathematical and theoretical aspects of Kautz filters are more interesting for academic purposed, some practical applications can be found in the literature. For example, the flight testing certification of aircrafts for aeroelastic stability was completely charecterized through a series connection of Kautz filters in [1]. The application used a simulated nonlinear prototypical two-dimensional wing section and F/A-18 active aeroelastic wing ground vibration test data.

In specific control applications with Kautz filters, the strategies are, normally, based on active noise control using feedforward compensation, e. g. as performed in [26]. It is well-known that Wiener theory can be used to describe internal model control to change the control architecture from feedforward to feedback [3]. However, feedback compensation can also be directly implemented. Thus, the goal of the present chapter is to apply Kautz filters for active vibration control. The main steps and characteristics involved in this procedure are described. Specifically, this chapter emphasises the following:

- Feedback control, considering dynamic canceling.
- It is not necessary to have a complete mathematical model and the controller is designed directly in the digital domain for fast practical implementation.
- The control method is based on experimental IRFs (nonparametric) and in orthonormal basis functions. Thus, the method is grey-box because prior knowledge of the mechanical vibrating system treated is assumed (poles of Kautz filter to represent the system). Additionally, complex vibration system can be controlled.
- An example of a single-degree of freedom mechanical model is used to illustrate the main steps.
- Additionally, an experimental example by using a clamped beam with PZT actuator and PVDF sensor is presented.

The chapter is organized as follows. First, the IRF identification and covariance method is reviewed briefly, followed by the Kautz filter with multiple poles for expansion of impulse response. After, a vibration control strategy is described and example applications involving single-input-single-output vibrating systems are used to illustrate the approach. Finally, the results are discussed and suggestions for a non-linear identification procedure are proposed.

2. Impulse response function

The output $\tilde{y}(k)$ of a linear discrete-time and invariant system can be written as:

$$\tilde{y}(k) = \sum_{i=0}^{\infty} h(i)u(k-i) \tag{1}$$

where the sequences $\{u(k), k = 0, 1, \ldots, T_f\}$ and $\{\tilde{y}(k), k = 0, 1 \ldots, T_f\}$ are the sampled input and output signals, respectively; T_f is the final time, and $h(k)$ is the impulse response function

(IRF). The measured output signal is given by $y(k) = \tilde{y}(k) + w(k)$, where $w(k)$ is a white or colored noise. The eq. (1) represents a sum of convolution between the input signal $u(k)$ and the IRF $h(k)$. In mechanical and vibrating systems applications, the IRF can be obtained by impact tests with a hammer or by using numerical algorithms based on time or frequency measured signals.

Normally, to obtain the IRF, eq. (1), is truncated in N terms by considering $|h(k)| < \epsilon, \forall j > N$, where ϵ is a residue. In this case, eq. (1) can be given as:

$$y(k) \approx \sum_{i=0}^{N} h(i)u(k-i) \tag{2}$$

The approach in eq. (2) changes an infinite impulse response model (IIR) into a finite impulse response model (FIR). The most common method to identify the $h(k)$ is by using the correlation functions due to the robustness to noise issues yielding to the classical Wiener-Hopf equation:

$$R_{uy}(k) \approx \sum_{i=0}^{N} h(i)R_{uu}(k-i) \tag{3}$$

where the correlation function $R_{uu}(k)$ and cross-correlation function $R_{uy}(k)$ can be estimated experimentally. Based on eq. (3), a least-square (LS) identification method can be performed to estimate the expansion coefficients in the time-series that describes the FIR model $h(k)$. This approach for estimating an IRF has some advantages over other estimators, for instance:

- the stability of the identified model is guaranteed a priori, since the model is FIR.
- the model is assumed to be described only for arbitrary zeros and poles at the origin of the complex plane.
- the model is linear in the parameters, hence the LS approach can be performed.

However, this identification technique often leads to conservative results because a common vibration system is hardly ever represented by a FIR model. Thus, the practical drawback is that a large number of parameters $h(k)$ must be considered in order to obtain a good approach in eq. (3). In order to overcome this drawback, a set of orthonormal basis functions can be employed to expand the covariance method and reduces the number of parameters. Next section provides some considerations in this sense.

3. Covariance method expanded in orthonormal basis functions

The IRF $h(k)$ can alternatively be written using α_j, $j = 0, 1, \ldots, J$, as expansion coefficients described by z-function $\Psi_j(z)$:

$$h(k) = \sum_{j=0}^{J} \alpha_j \psi_j(k), \qquad k = 0, 1, \ldots, N \tag{4}$$

where $\psi_j(k)$ is the IRF of the transfer function $\Psi_j(z)$. The z transform of eq. (4) is given by a linear combination of the functions $\Psi_j(z)$:

$$H(z) \approx \alpha_0\Psi_0(z) + \alpha_1\Psi_1(z) + \cdots + \alpha_J\Psi_J(z) = \sum_{j=0}^{J} \alpha_j\Psi_j(z) \tag{5}$$

The convergence of $\Psi_j(z)$ is related to the completeness properties of these subsets of functions. If the functions $\Psi_j(z)$ are properly chosen (poles placement), the order $J << N$. Thus, it is easier to identify the coefficient α_j using eq. (4) [2, 12, 14, 15, 22, 24], which can be written in a matrix form:

$$\begin{Bmatrix} h(0) \\ h(1) \\ \vdots \\ h(N) \end{Bmatrix} = \begin{bmatrix} \psi_0(0) & \psi_1(0) & \cdots & \psi_J(0) \\ \psi_0(1) & \psi_1(1) & \cdots & \psi_J(1) \\ \vdots & \vdots & \ddots & \vdots \\ \psi_0(N) & \psi_1(N) & \cdots & \psi_J(N) \end{bmatrix} \begin{Bmatrix} \alpha_0 \\ \alpha_1 \\ \vdots \\ \alpha_J \end{Bmatrix} \tag{6}$$

By incorporating the eq. (4) into Wiener-Hopf equation, eq. (3), one can obtain:

$$\begin{aligned} R_{uy}(k) &\approx \sum_{i=0}^{N} h(i)R_{uu}(k-i) \equiv \sum_{i=0}^{N}\sum_{j=0}^{J} \alpha_j\psi_j(i)R_{uu}(k-i) \\ &= \sum_{j=0}^{J} \alpha_j \sum_{i=0}^{N} \psi_j(i)R_{uu}(k-i) = \sum_{j=0}^{J} \alpha_j v_j(k) \end{aligned} \tag{7}$$

where $v_j(k)$, $k = 0, \cdots, N$ is the input signal $R_{uu}(k)$ processed by each element of the discrete-time function $\psi_j(k)$, $j = 0, 1, \ldots, J$, which forms the approximation base and is the IRF of the orthogonal function:

$$v_j(k) = \sum_{i=0}^{N} \psi_j(i)R_{uu}(k-i) \tag{8}$$

Eq. (8) is basically a filtering of the input signal $R_{uu}(k)$ by a set of filter $\psi_j(k)$. Finally, the eq. (7) is used to describe:

$$\begin{Bmatrix} R_{uy}(0) \\ R_{uy}(1) \\ \vdots \\ R_{uy}(N) \end{Bmatrix} = \begin{bmatrix} v_0(0) & v_1(0) & \cdots & v_J(0) \\ v_0(1) & v_1(1) & \cdots & v_J(1) \\ \vdots & \vdots & \ddots & \vdots \\ v_0(N) & v_1(N) & \cdots & v_J(N) \end{bmatrix} \begin{Bmatrix} \alpha_0 \\ \alpha_1 \\ \vdots \\ \alpha_J \end{Bmatrix} \tag{9}$$

The effectiveness of the model is limited by the choice of the filters $\Psi_j(z)$. Thus, the choice of the basis functions is very important. For describing mechanical vibration and flexible systems, the Kautz functions have been demonstrated to provide a good generalization by including complex poles in the z-domain [2, 14].

4. Kautz filter

The Kautz filters can be given by [16, 22, 24]:

$$\Psi_{2n}(z) = \frac{\sqrt{(1-c^2)(1-b^2)}z}{z^2+b(c-1)z-c}\left[\frac{-cz^2+b(c-1)z+1}{z^2+b(c-1)z-c}\right]^{n-1} \tag{10}$$

$$\Psi_{2n-1}(z) = \frac{\sqrt{1-c^2}z(z-b)}{z^2+b(c-1)z-c}\left[\frac{-cz^2+b(c-1)z+1}{z^2+b(c-1)z-c}\right]^{n-1} \tag{11}$$

where the constants b and c are relative to the poles $\beta = \sigma + j\omega$ and $\beta^* = \sigma - j\omega$ in the j-th filter through the relations:

$$b = \frac{(\beta_j + \beta_j^*)}{(1+\beta_j\beta_j^*)}, \tag{12}$$

$$c = -\beta\beta_j^* \tag{13}$$

A sequence of filters is utilized with different poles in each section describing the modal behavior in the frequency range of interest. A question is relative for choosing the poles and the IRFs iteratively based on application of eq. (2) and output experimental signal $y_e(k)$. An error signal can be written by:

$$e(k) = \hat{y}(k) - y_e(k) \tag{14}$$

where $\hat{y}(k)$ is the predicted output signal by the IRF $\hat{h}(k)$ estimated considering Kautz basis defined by the poles β_j and β_j^* in the z-domain:

$$\hat{y}(k) = \sum_{i=0}^{N} \hat{h}(i)u(k-i) \tag{15}$$

The optimization problem can be described by objective function that employs an Euclidean norm and the Kautz poles are functions of the frequencies and damping factors that are the optimization parameters. These parameters can be restricted in a range searching. This optimization problem can be solved by several classical approaches. A detailed explanation in this point can be found in [12].

5. Active vibration control strategy

If an IRF is well identified through covariance method expanded with Kautz filters, a model in z-domain can be described by applying the $z-$ transform in the IRF $h(k)$[1]:

$$H(z) = \sum_{n=0}^{+\infty} h(n)z^{-n} \approx \alpha_0\Psi_0(z) + \alpha_1\Psi_1(z) + \cdots + \alpha_J\Psi_J(z) \tag{16}$$

[1] Considering $h(k)$ is a causal sequence.

A controller can be inserted in the direct branch of the control loop to try to reject the disturbance. This controller $G(z)$ has a digital structure given by:

$$G(z) = L(z)H^{-1}(z) \tag{17}$$

where $H^{-1}(z)$ is the inverse of the identified transfer function of the system and $L(z)$ has the desirable dynamic. The compensator $L(z)$ can have a second order structure or any format with a damping ratio ξ_c bigger than the uncontrolled damping ratio. The control project is to find a gain and the $G(z)$ formed to reduce the damping of the system. For practical implementation, these equations can be programmed directly in the discrete-time domain by using the mathematical convolution operator.

It is worth to point out that one consider only the control of stable systems described by $H(z)$ experimentally identified. Consequently, the transfer function $H(z)$ has all poles within the unitary circle because $H(z)$ is identified using the Kautz poles that are set to be stable. The auxiliary function $L(z)$ is proposed to warrant stability and the required performance in the closed-loop system

Two examples are used to show the approach proposed. The first one is a single-degree-of-freedom model that is a simple and easy example for the interested reader reproduce it. The second one is based on active vibration control in a smart structure with PZT actuator and PVDF sensor for presenting its use employing experimental data.

The results are illustrated in a single-degree-of-freedom model given by:

$$\ddot{x}(t) + 2\xi\omega_n\dot{x}(t) + \omega_n^2 x(t) = f(t) \tag{18}$$

where $x(t)$ is the displacement vector, the over dot is the time derivative, ξ is the damping factor, ω_n is the natural frequency in rad/s and $f(t)$ is the excitation force. To simulate the uncontrolled responses, it were used the values of $\xi = 0.01$ and $\omega_n = 62.83$ rad/s that correspond to 10 Hz. The motion equation from eq. (18) is solved numerically through the Runge-Kutta method with a sampling rate of 100 Hz, that corresponds to a time sample of $dt = 0.01$ s, with 2048 samples. The force used was a white noise random with level of amplitude of the 3 N. The fig. (1) shows the input and output signal simulated for uncontrolled condition.

An important step to identify the IRFs is the choice of Kautz poles that need to reflect adequately the dominant dynamics of the vibrating systems. In real-world application the choice of the poles is a complicated problem. However, a simple power spectral density of the output signal (in our example the displacement) can give an orientation to help in the selection. If the system is more complicated, an optimization procedure could be used [12]. Figure (2) shows the power spectral density of the displacement. Clearly, it seems a peak value close to 10 Hz that is a possible candidate of natural frequency. The frequency response function (FRF) experimental is also estimated through spectral analysis only to compare the values of the natural frequency and damping factor, fig. (3).

Based on the frequency of 10 Hz, a continuous pole in $s-$domain given by $s_{1,2} = -0.6283 \pm 62.82j$, where j is the imaginary unit, is set. Kautz filter is described in discrete-time domain, so, it is necessary to convert the pole to $z-$domain. The relationship $\beta = e^{sdt}$ can be used to

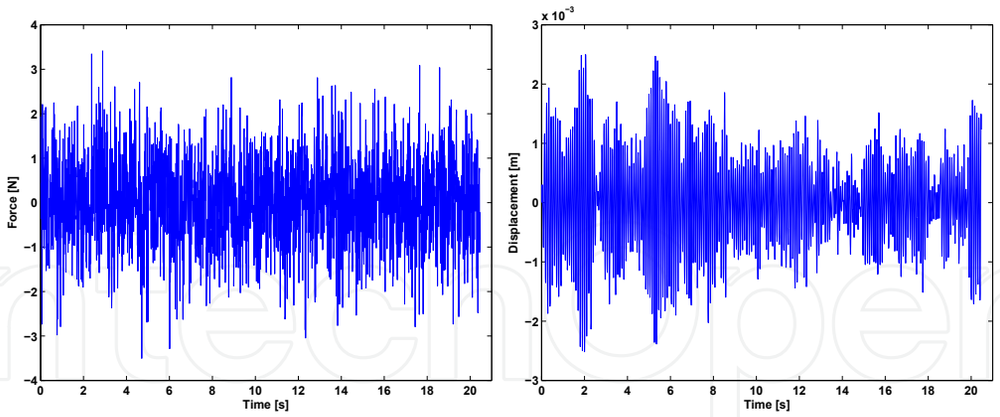

(a) Input force (disturbance). (b) Output displacement.

Figure 1. Response of the system for the uncontrolled case.

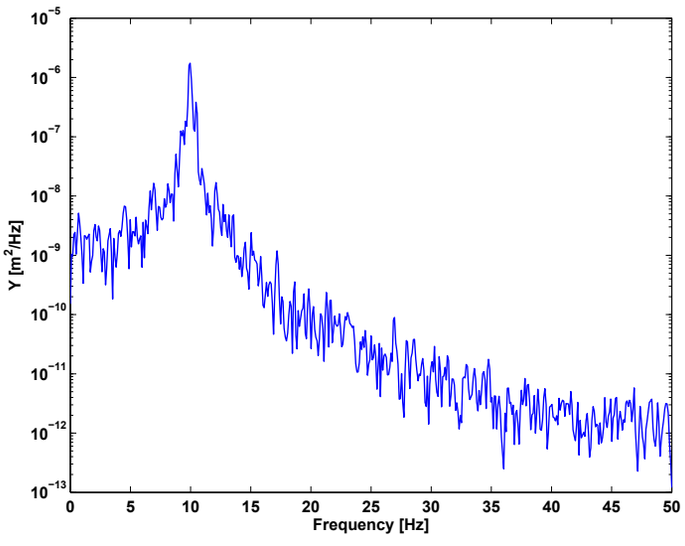

Figure 2. Power spectral density of the output signal (displacement) estimated using Welch method with Hanning window, 25 % of overlap and two sections.

obtain the discrete Kautz poles given by $\beta = 0.8040 + 0.5841j$ and $\beta^* = 0.8040 + 0.5841j$. Once the system is a SISO and with only one degree of freedom, only one section of Kautz filter is employed, $J = 1$ (2 terms), and $N = 600$ samples are considered to be enough to complete description of the memory lag. The constants b and c are computed through eq. (12) and (13) and the eqs. (10) and (11) are utilized to construct the Kautz filter given by:

$$\Psi_0(z) = \frac{0.0926}{z^2 - 1.608z + 0.9875} \tag{19}$$

$$\Psi_1(z) = \frac{0.1575z - 0.1275}{z^2 - 1.608z + 0.9875} \tag{20}$$

The impulse response of the two sections of the Kautz filter are used to process the correlation function of the input signal $f(t)$, through eq. (8). Equation (9) is solved by LS approach in

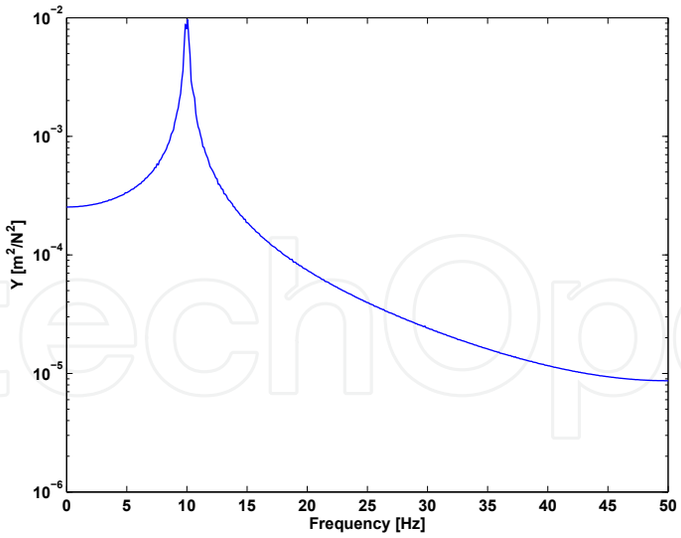

Figure 3. Frequency response function identified using spectral estimate H_1 through Welch method with Hanning window, 25 % of overlap and two sections.

order to identify the expansion coefficients α_0 and α_1. With these values, eq. (6) is used to identify the IRF. Figure (4) presents the result of the identification process and compare with the analytical IRF. It is observed a good concordance between the experimental identified and the theoretical IRF.

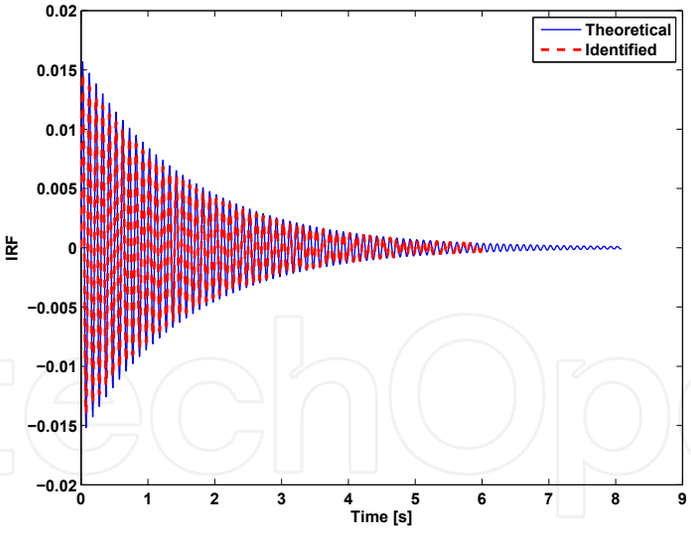

Figure 4. Impulse response function comparison between analytical and identified by Kautz filters.

Once the IRF is identified, an experimental FIR model representative of the system is now known. This $H(z)$ model is used to represent a controller $G(z)$ inserted in the direct branch of the control loop with unitary feedback, by using the following expression:

$$G(z) = L(z)H^{-1}(z) \tag{21}$$

where $H^{-1}(z)$ is the inverse of the transfer function of the system identified experimentally, $H(z)$, described by:

$$H(z) \approx \alpha_0 \Psi_0(z) + \alpha_1 \Psi_1(z) \tag{22}$$

and $L(z)$ is a desirable dynamic to the system. The controller used has the following structure of a second order system:

$$L(s) = K \frac{\omega_n^2}{s^2 + 2\xi_c \omega_n s + \omega_n^2} \tag{23}$$

where ξ_c is the damping factor of the controlled system and K is a control gain. The structure in eq. (23) is continuous in the $s-$domain, and for application in a digital format is necessary to use a bilinear transform (Tustin's method). It is chosen a gain of $K = 3 \times 10^{-4}$ and $\xi_c = 0.08$. These values are chosen based on the adequate behavior for the controlled system in the closed loop and with a low level of control actuator force required. The natural frequency in closed loop is maintained the same of the uncontrolled system. Thus, the digital compensator $L(z)$ is given by:

$$L(z) = 10^{-5} \frac{5.543z + 5.358}{z^2 - 1.541z + 0.9044} \tag{24}$$

Finally, the feedback transfer function $M(z)$ is given by:

$$M(z) = \frac{L(z)H^{-1}(z)H(z)}{1 + L(z)H^{-1}(z)H(z)} \tag{25}$$

that corresponds to:

$$M(z) = 10^{-5} \frac{5.543z^3 - 3.184z^2 - 3.244z + 4.846}{z^4 - 3.082z^3 + 4.183z^2 - 2.787z + 0.8179} \tag{26}$$

Clearly the effectiveness of the controller depends on the correct identification of the $H(z)$ to allow a perfect cancelation. Figure (5) shows the frequency response function comparison between uncontrolled and controlled system where it is seen that the peak decrease by increase actively the damping with the digital compensator. Figure (6) shows the output displacement without and with control. The disturbance force is considered with the same level and type of the tests used in the uncontrolled condition.

A cantilever aluminium beam with a PZT actuator patch and a piezoelectric sensor (PVDF) symmetrically bonded to both sides of the beam is used to illustrate the process of IRF identification and design of a digital controller for active vibration reduction. The PZT and PVDF are bonded attached collocated near to the clamped end of the beam, as seen in fig. (7). The PZT patch is the model QP10N from ACX with size of $50 \times 20 \times 0.254$ mm of length, width and thickness, respectively. The PVDF has dimensions of $30 \times 10 \times 0.205$ mm of length, width and thickness, respectively, and it is bonded with a distance of 5 mm of the clamped end. The complete experimental setup is shown in figs. (7) and (8).

A white noise signal is generated in the computer, converted to analogic domain with a D/A converter and pre-processed by a voltage amplifier with gain of 20 V/V before application in the PZT actuator. The output signal is measured with the PVDF and linked directly with the

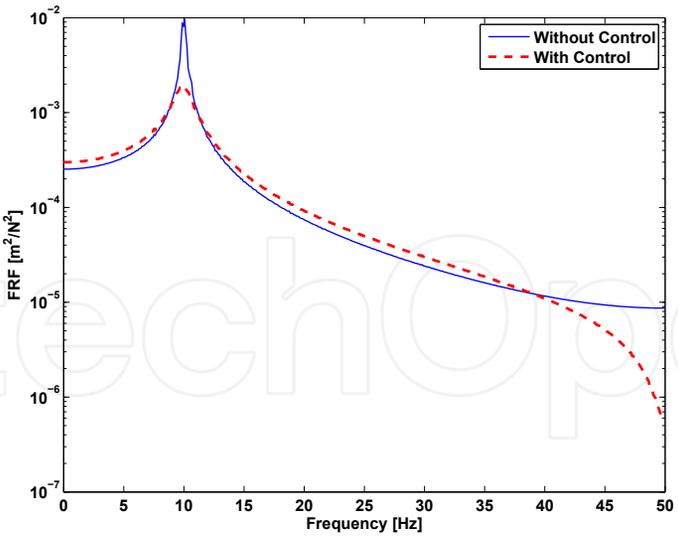

Figure 5. Frequency response function comparison between uncontrolled and controlled condition.

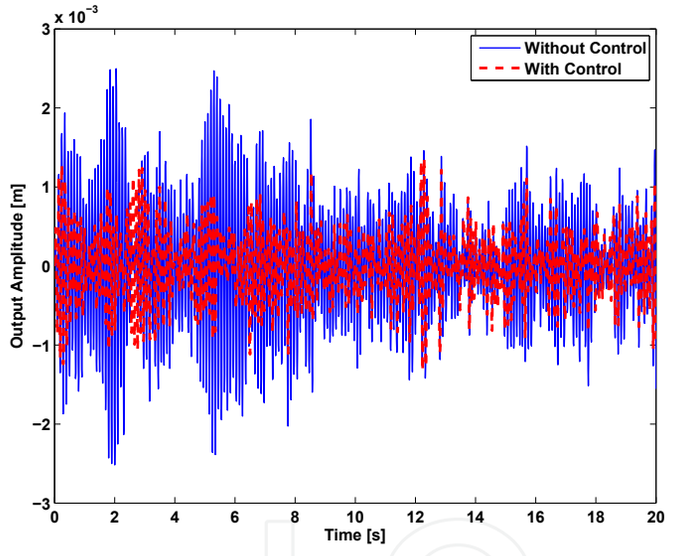

Figure 6. Output displacement comparison between uncontrolled and controlled condition.

charge amplifier and pre-processed with a A/D converter. All experimental signals are saved and processed with a *dSPACE* 1104 acquisition board with a sample rate of 1 kHz and with 5 seconds of test duration. Figure (9) shows the time series signals of PZT actuator (input) and PVDF sensor (output) for uncontrolled system.

The first step in this approach is the choosing an adequate set of poles for the Kautz Filters. As the mathematical model is unknown, one needs to start by availing the power spectral density of the PVDF sensor (output) as suggested in the first example. Figure (10) presents the power spectral density of the output signal (PVDF) estimated using Welch method with Hanning window, 50 % of overlap and 5 sections. The peaks in frequencies of 13, 78, 211, 355 and 434 Hz can be considered candidates for natural frequencies. For comparison purposes,

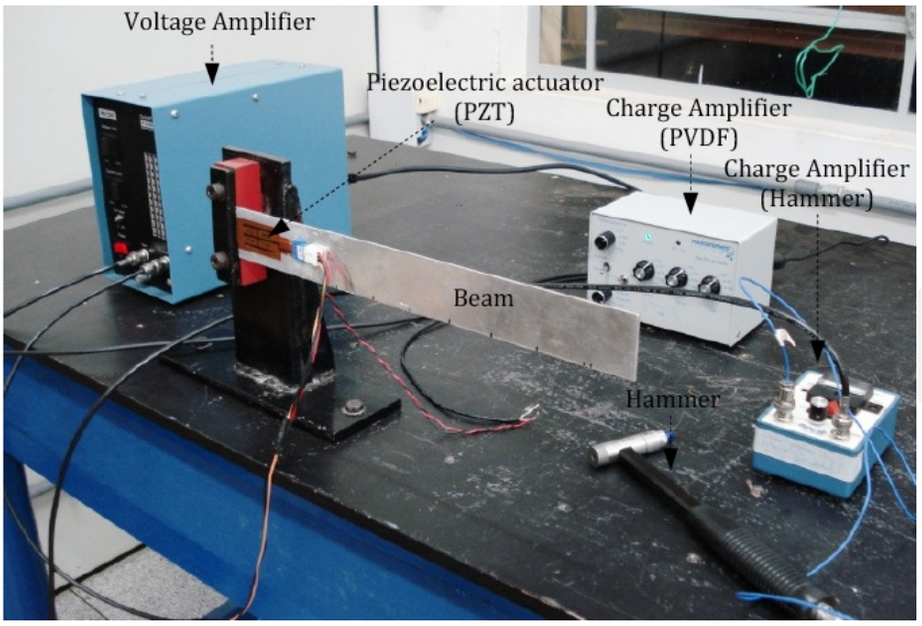

(a) Overall experimental setup.

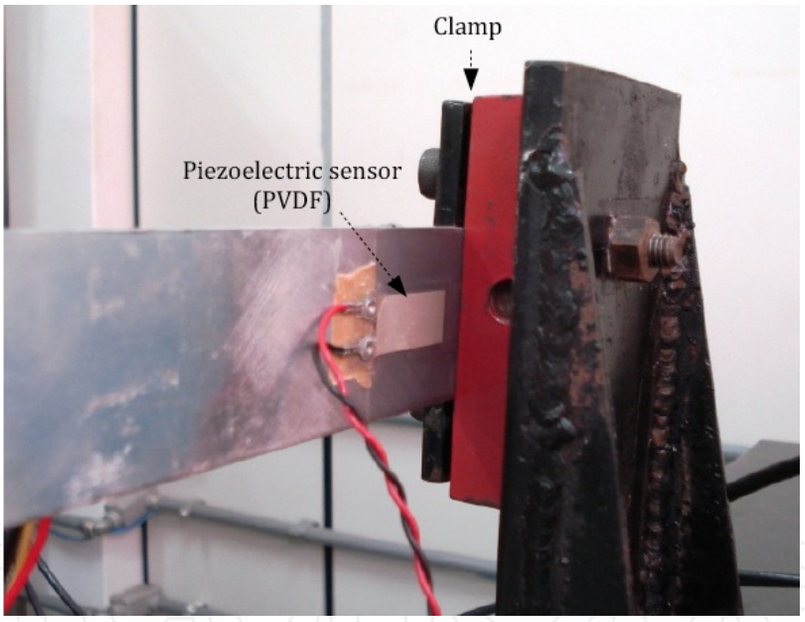

(b) Detail of the PVDF Sensor.

Figure 7. View of the experimental setup.

the frequency response function (FRF) experimental is estimated through spectral analysis to observe the values of the natural frequencies and damping factors, fig. (11).

Based on the spectral analysis one must choose the continuous poles candidates given by $s_i = -\xi_i\omega_{ni} \pm j\omega_{ni}\sqrt{1-\xi_i^2}$, $i = 1,2,3,4,5$. The most difficult parameters to be identified are the damping factors. Several trial and error tests were performed until to reach an adequate

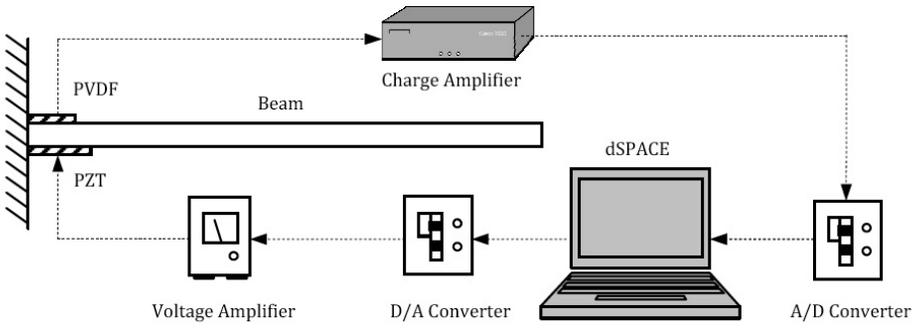

Figure 8. Experimental setup.

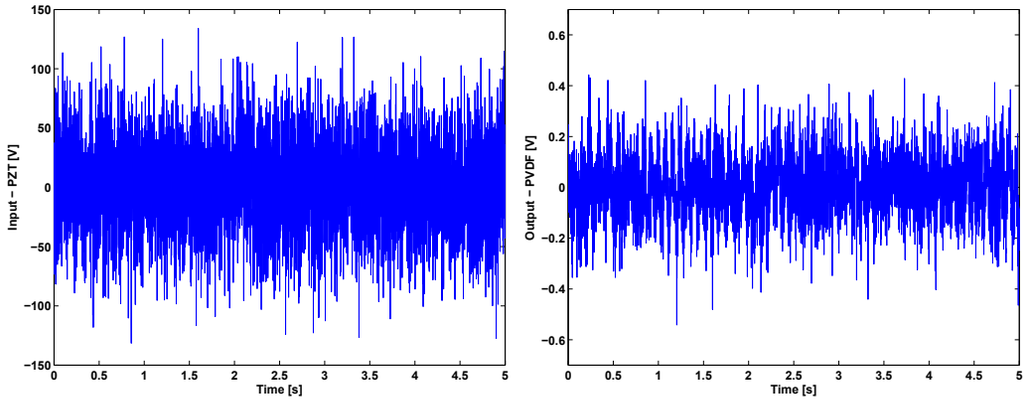

(a) PZT Actuator. (b) PVDF Sensor.

Figure 9. Response of the experimental tests in the time domain for the uncontrolled case.

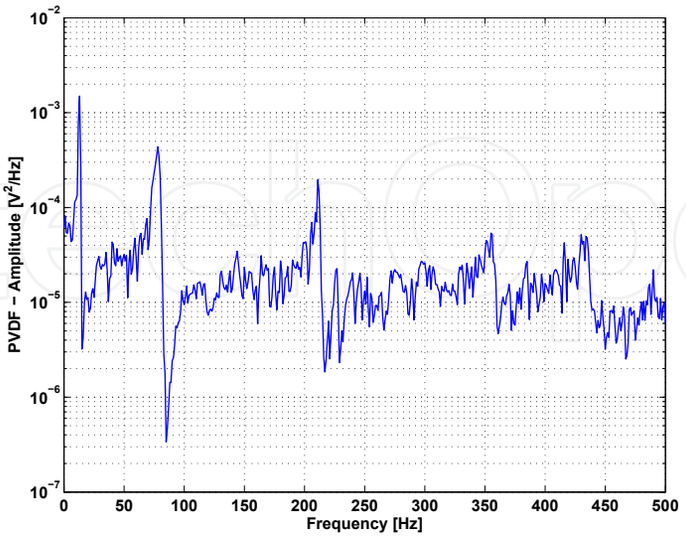

Figure 10. Power spectral density of the output signal (PVDF) estimated using Welch method with Hanning window, 50 % of overlap and 5 sections.

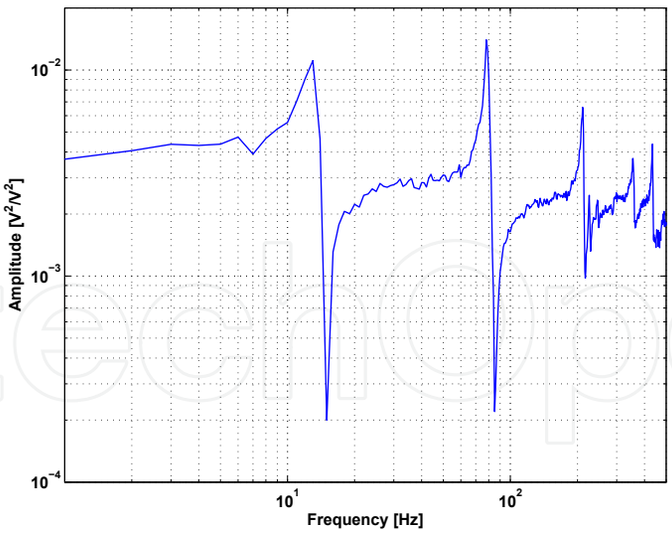

Figure 11. Frequency response function identified using spectral estimate H_1 through Welch method with Hanning window, 50 % of overlap and 5 sections.

result. A reasonable identification were reached based on the parameters given by:

$$\omega_{n1} = 81.68 \quad \text{rad/s} \qquad \xi_1 = 0.04 \qquad s_1 = -3.2673 \pm 81.6160j \tag{27}$$

$$\omega_{n2} = 490.08 \quad \text{rad/s} \qquad \xi_2 = 0.019 \qquad s_2 = -9.3117 \pm 490j \tag{28}$$

$$\omega_{n3} = 1.3258 \times 10^3 \quad \text{rad/s} \qquad \xi_3 = 0.02 \qquad s_3 = -26.515 \pm 1325.5j \tag{29}$$

$$\omega_{n4} = 2.23 \times 10^3 \quad \text{rad/s} \qquad \xi_4 = 0.1 \qquad s_4 = -223.05 \pm 2219.4j \tag{30}$$

$$\omega_{n5} = 2.72 \times 10^3 \quad \text{rad/s} \qquad \xi_5 = 0.1 \qquad s_5 = -276.7 \pm 2713.2j \tag{31}$$

Once the fourth and fifth modes are apparently well damped by analysing the frequency response the correspond poles are also considered well damped (not dominants). The Kautz filter is described in the discrete-time domain. So, it is necessary to convert to $z-$domain. The relationship $\beta_i = e^{s_i dt}$ can be used to obtain the five pair of complex discrete Kautz poles given by:

$$\beta_1 = 0.9934 \pm 0.0813j \tag{32}$$

$$\beta_2 = 0.8742 \pm 0.4663j \tag{33}$$

$$\beta_3 = 0.2365 \pm 0.9447j \tag{34}$$

$$\beta_4 = -0.4833 \pm 0.6376j \tag{35}$$

$$\beta_5 = -0.6925 \pm 0.3163j \tag{36}$$

The cantilever beam is a SISO system, but with apparent five modes in the frequency range computed of interest. So, they are used 5 sections of Kautz filters, $J = 4$ and $N = 1200$ samples that are considered to be enough to complete the view of the memory lag. The constants b and c are computed and the eqs. (10) and (11) are utilized to construct the Kautz filters.

Figure (12) shows the comparison between the IFFT of the FRF from H_1 estimated and the IRF identified through Kautz filter.

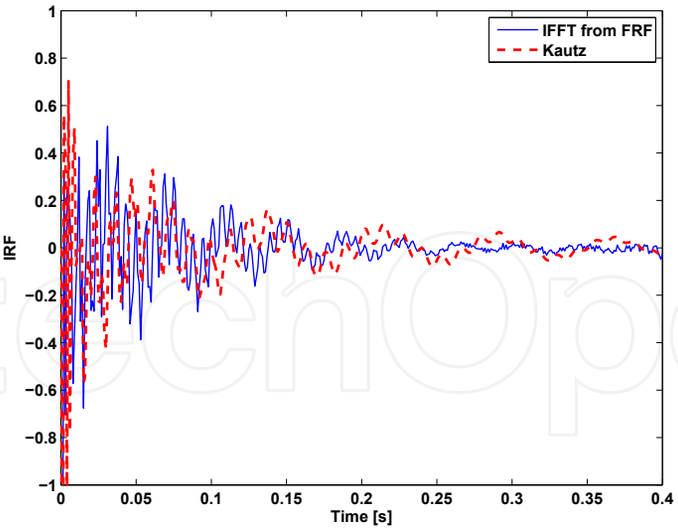

Figure 12. Impulse response function comparison between IFFT of the estimated FRF and identified by Kautz filters.

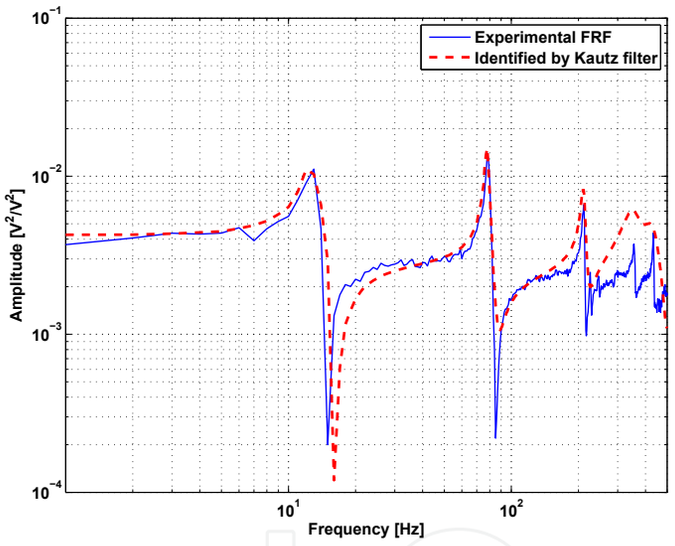

Figure 13. FRF comparison between estimated FRF through H_1 spectral estimate and identified by Kautz filters.

Although, it seems that are not a complete visual agreement between the curves, the FRF seen in figure (13) presents a good agreement. It is worth to comments that with the same experimental data, [23] identified a state-space model through Eigensystem Realization Algorithms (ERA) combined with Observer/Kalman filter Identification (OKID). The results presented with Kautz filter allowed a better identification in this frequency range comparing than with ERA/OKID.

Figure (14) shows the output response of th PVDF estimated by a convolution between the IRF identified by Kautz filter with the input excitation from PZT actuator. The estimated output can be compared with the experimental measured response (see fig. 9(b)).

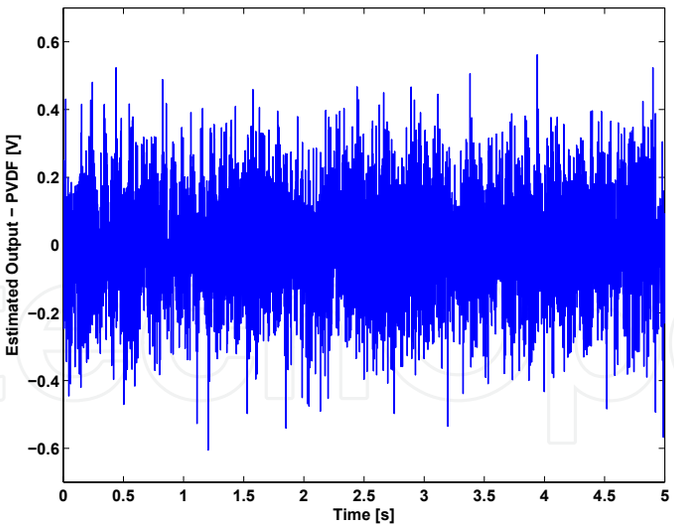

Figure 14. PVDF output estimated by IRF identified with Kautz filters.

The controller is designed based on the inverse of the identified system described by eq. (16), called by $H^{-1}(z)$, in series with a compensator $L(z)$. The $L(z)$ is chosen by combination of 3 second-order system realized in parallel structure:

$$L(z) = K\left(L_1(z) + L_2(z) + L_3(z)\right) \tag{37}$$

where $K = 1.5 \times 10^{-3}$ is a controller gain and the transfer functions are defined by:

$$L_1(z) = \frac{0.003316z + 0.003298}{z^2 - 1.977z + 0.9838} \tag{38}$$

$$L_2(z) = \frac{0.1122z + 0.1068}{z^2 - 1.644z + 0.8633} \tag{39}$$

$$L_3(z) = \frac{0.6691z + 0.5813}{z^2 - 0.4215z + 0.6718} \tag{40}$$

It is important to observe that the three compensators, $L_1(z)$, $L_2(z)$ and $L_3(z)$ have the natural frequencies corresponding to the first three modes of the systems, but with an increase in the level of damping factor for reducing the vibration level in the closed-loop system. The compensator $L(z)$ in its final form is given by:

$$L(z) = \frac{0.001177z^5 - 0.003011z^4 + 0.001994z^3 + 0.001218z^2 - 0.002219z + 0.0008492}{z^6 - 4.043z^5 + 7.297z^4 - 7.907z^3 + 5.676z^2 - 2.592z + 0.5706} \tag{41}$$

It was decided to control only the 3 first modes for two main reasons:

- The fourth and fifth modes are not dominant.
- Additionally, these modes are not well identified by the Kautz filter. One included the damping factor in these modes with these values shown above in order to correct identification the anti-ressonance region.

Figure (15) shows the FRF comparison between the uncontrolled (estimated by Kautz filter) and controlled system where is possible to observe the reduction in the resonance peak caused by the controller implemented.

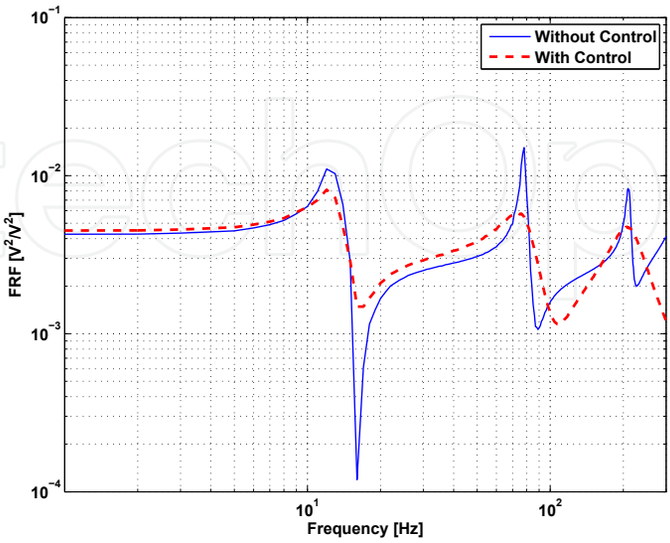

Figure 15. FRF comparison between uncontrolled and controlled condition. Input: PZT actuator - Output: PVDF sensor.

Another advantage of this procedure face to state-feedback approaches is relative to the controlability and observability conditions. If one use procedures identification for obtaining a state-space realization, e. g. ERA/OKID as made by [23], is necessary to verify a prior the observability and controlability conditions. In some situations some modes are not controllable and observable adequately with a specific realization. Once the technique used in this chapter is not described in state-space variables and it is based on input/output variables with non-parametric IRF model, these kinds of drawbacks are avoided.

This chapter has described a procedure for non-parametric system identification of an impulse response function (IRF) based on input and output experimental data. Orthogonal functions are used to reduce the number of samples to be identified. A simple active vibration control procedure with a digital compensator that seeks to cancel the plant dynamic is also described. Once the IRF in the uncontrolled condition is well estimated by Kautz filters, the control strategy presented can increase the damping in a satisfactory level with low actuator requirements. Single-input-single-output vibrating systems have been used to illustrate the performance and the main aspects for practical implementation. This procedure can also be extended for nonlinear systems using Hammerstein or Wiener block-oriented models.

Acknowledgements

The authors are thankful for the financial support provided by National Council for Scientific and Technological Development (CNPq/Brasil), INCT and São Paulo Research Foundation (FAPESP). The authors acknowledge the helpful suggestions of the Editor. The authors also are thankful the help of Prof. Dr. Gustavo Luiz Chagas ManhŃes de Abreu and Sanderson Manoel da Conceição for providing the experimental data in the clamped beam.

Author details

Samuel da Silva, Vicente Lopes Junior and Michael J. Brennan
UNESP - Univ Estadual Paulista, Faculdade de Engenharia de Ilha Solteira, Departamento de Engenharia Mecânica, Av. Brasil 56, Centro, Ilha Solteira, SP, Brasil

6. References

[1] Baldelli, D. H., Lind, R. & Brenner, M. [2005]. Nonlinear aeroelastic/aeroservoelastic modeling by block-oriented identification, *Journal of Guidance, Control and Dynamics* 28(5): 1056–1064.

[2] Baldelli, D. H., Mazzaro, M. C. & Peña, R. S. S. [2001]. Robust identification of lightly damped flexible structures by means of orthonormal bases, *IEEE Transactions on Control Systems Technology* 9(5): 696–707.

[3] Brennan, M. J. & Kim, S. M. [2001]. Feedforward and feedback control of sound and vibration - a Wiener filter approach, *Journal of Sound and Vibration* 246(2): 281–296.

[4] Brinker, A. C. & Belt, H. J. W. [1998]. Using kautz models in model reduction, *in* A. Prochazka, J. Uhlír, P. J. W. Rayner & N. Kingsbury (eds), *Signal Analysis and prediction*, 1st edn, Birkhauser Boston.

[5] Campello, R. J. G. B., Oliveira, G. H. C. & Amaral, W. C. [2007]. Identificação e controle de processos via desenvolvimento em séries ortonormais. parte a: Identificação, *Revista Controle & Automação* 18(3): 301–321.

[6] D. Mayer, S. H. H. H. [2001]. Application of Kautz models for adaptive vibration control, *in* IMECE (ed.), *American Society of Mechanical Engineers (Veranst.)*, ASME International Mechanical Engineering Congress and Exposition, NewYork.

[7] da Rosa, A., Campello, R. J. G. B. & do Amaral, W. C. [2006]. Desenvolvimento de modelos de Volterra usando funções de Kautz e sua aplicação à modelagem de um sistema de levitaçãoo magnética, *XVI Congresso Brasileiro de Automática*.

[8] da Rosa, A., Campello, R. J. G. B. & do Amaral, W. C. [2007]. Choice of free parameters of discrete-time Volterra models using Kautz functions, *Automatica* 43(6): 1084–1091.

[9] da Rosa, A., Campello, R. J. G. B. & do Amaral, W. C. [2008]. An optimal expansion of Volterra models using independent Kautz bases for each kernel dimension, *International Journal of Control* 81(6): 962–975.

[10] da Rosa, A., Campello, R. J. G. B. & do Amaral, W. C. [2009]. Exact search directions for optimization of linear and nonlinear models based on generalized orthonormal functions, *IEEE Transactions os Automatic Control* 54(12): 2757–2772.

[11] da Silva, S. [2011a]. Non-linear model updating of a three-dimensional portal frame based on Wiener series, *International Journal of Non-linear Mechanics* 46: 312–320.

[12] da Silva, S. [2011b]. Non-parametric identification of mechanical systems by Kautz filter with multiple poles, *Mechanical Systems and Signal Processing* 25(4): 1103–1111.

[13] da Silva, S., Cogan, S. & Foltête, E. [2010]. Nonlinear identification in estructural dynamics based on Wiener series and Kautz filter., *Mechanical Systems and Signal Processing* 24(1): 52–58.

[14] da Silva, S., Dias Júnior, M. & Lopes Junior, V. [2009]. Identification of mechanical systems through Kautz filter, *Journal of Vibration and Control* 15(6): 849–865.

[15] Heuberger, P. S. C., Van Den Hof, P. M. J. & Wahlberg, B. [2005]. *Modelling and Identification with Rational Orthogonal Basis Functions*, 1st edn, Springer.
[16] Heuberger, P., Van Den Hof, P. & Bosgra, O. H. [1995]. A generalized orthonormal basis of linear dynamical systems, *IEE Transactions on Automatic Control* 40(3): 451–465.
[17] Kautz, W. H. [1954]. Transient synthesis in the time domain, *IRE Transactions on Circuit Theory* 1(1): 29 – 39.
[18] Oliveira, G. H. C., Amaral, W. C., Favier, G. & Dumont, G. A. [2000]. Constrained robust predictive controller for uncertain processes modeled by orthonormal series functions, *Automatica* 36(4): 563–571.
[19] Oliveira, G. H. C., Campello, R. J. G. B. & Amaral, W. C. [2007]. Identificação e controle de processor via desenvolvimento em séries ortonormais. parte b: Controle preditivo, *Revista Controle & Automática* 18(3): 322–336.
[20] Paetero, T. & Karjalainen, M. [2003]. Kautz filters and generalized frequency resolution: Theory and audio aplications, *Audio Engineering Society* 51(1/2): 27–44.
[21] Sansone, G. [1958]. *Orthogonal Functions*, Vol. 9, Dover Publications.
[22] Van Den Hof, P. M. J., Heuberger, P. S. & Bokor, J. [1995]. System identification with generalized orthonormal basis functions, *Automatica* 31(12): 1821–1834.
[23] Vasques, C. H., Conceição, S. M., Abreu, G. L. C. M., Lopes Jr., V. & Brennan, M. J. [2011]. Identification and control of systems submitted to mechanical vibration, *21st International Congress of Mechanical Engineering - COBEM 2011*, Natal, RN, Brasil.
[24] Wahlberg, B. [1994]. System identification using Kautz models, *IEEE Transactions on Automatic Control* 39(6): 1276 – 1282.
[25] Wahlberg, B. & Makila, P. M. [1996]. On approximation of stable linear dynamical systems using Laguerre and Kautz functions, *Automatica* 32(5): 693–708.
[26] Zeng, J. & de Callafon, R. [2005]. Filters parametrized by orthonormal basis functions for active noise control, *ASME International Mechanical Engineering Congress and Exposition - IMECE 2005*.